Liquid – Liquid Crystalline Phase Separation in Biomolecular Solutions

Tommaso P. Fraccia[1]

Institut Pierre-Gilles de Gennes, CBI, ESPCI Paris, Université PSL, CNRS, 75005 Paris, France

Giuliano Zanchetta[2]

Dept. of Medical Biotechnology and Translational Medicine, University of Milano, Via Fratelli Cervi 93, 20090 Segrate, Italy

Abstract

Liquid-liquid phase separation (LLPS) and liquid crystalline (LC) ordering are ubiquitous phenomena in nature, in a variety of biomolecular solutions. Here we review instances in DNA, nanocellulose and other systems, where they occur together, leading to the formation of liquid-liquid crystalline phase separation (LLCPS), and we highlight analogies, differences, recent advances and open questions. Remarkably, the intrinsic fluid yet ordered nature of LC, combined with the spatial confinement induced by LLPS, leads to peculiar biomolecular compartments suitable for a broad range of applications, ranging from material science to synthetic biology. We argue that tools from the LC field help to address still unexplained processes such as the onset of phase transitions in intracellular biomolecular condensates.

Keywords: Lyotropic Liquid Crystals, Liquid-Liquid Phase Separations, Complex Coacervation, Biomolecular Condensates, Membraneless Organelles, DNA Self-Assembly, Molecular Crowding

1. Introduction

Phase separation is a ubiquitous and general phenomenon in colloidal dispersions and polymeric solutions, which takes place when a system gains free energy by de-mixing in two coexisting phases in thermodynamic equilibrium (1). In particular, the coexistence of two liquid phases, which takes the name of liquid-liquid phase separation (LLPS), has shown its relevance for material science applications, as a process to optimize the synthesis of nanomaterials with finely controlled properties (2; 3), and has currently revolutionized our understanding of intracellular organization and functioning (4; 5). Indeed, LLPS is a crucial mechanism regulating the formation and maturation of membraneless organelles, which are involved in tuning different cellular functions in physiology and disease (6; 7; 8). During the last decade, broad *in vitro* investigations of LLPS have been carried on to gain better knowledge on fundamental aspects of biomolecular condensation (9) and for the realization of functional and programmable synthetic compartments (10). Polymeric and colloidal systems are also prone to phase transitions from a homogeneous disordered liquid state to ordered crystals, amorphous arrested phases like gels or glasses and, under certain conditions, to liquid crystalline phases with orientational order (11; 12; 13).

Often, LLPS and phase transitions are intimately connected and in some cases also coupled to molecular self-assembly (14). For example, LLPS has long been exploited to control and trigger the appearance of a desired phase, otherwise difficult to access, such as the crystallization of proteins by polyethylene glycol (PEG) or Dextran aqueous two-phase-systems (15; 16), or to finely tune self-assembly processes by molecular crowding (17). In biological systems, liquid to solid transitions can modify, even irreversibly, the physical properties of intracellular biomolecular condensates, in turn affecting their proper biochemical functionality (6; 18; 19).

Liquid crystals (LC) are partially ordered states of matter in between disordered, isotropic (ISO) liquids and fully ordered crystalline states, which arise when molecules display sufficient anisotropy in shape or interactions (20; 21; 11). Besides thermotropic LC, the molecular fluids widely applied in display technology, there is the broad class of lyotropic LC, aqueous solutions of macromolecules spanning several orders of magnitude in molecular weight and dimensions, from surfactants and single nucleotides (nt) to cellulose nanocrystals (CNCs) to viruses (22; 23; 24).

In this review we highlight the numerous connections between LLPS and LC ordering, often unexpected for readers familiar with only one of the two fields, because we are convinced that many peculiar properties are yet to be discovered and explained. We will mainly focus on biomolecular, or biologically relevant, systems. We name this overlapping behaviour liquid-liquid crystal phase separation (LLCPS), a term recently used with slightly different meaning (25). We first give a brief overview on the different types of LLCPS in aqueous molecular mixtures through segregative or associative phase separation (26; 27). We then describe LLCPS in nucleic acids systems which have a strong relevance for biomolecular condensation (28). In the following sections, we present and

[1] tommaso.fraccia@espci.fr

[2] giuliano.zanchetta@unimi.it

discuss examples for other systems, namely chromonics, cellulose nanocrystals, actin and rod-like viruses. We will not cover other systems, like polymer dispersed liquid crystals, often prepared via polymerization-induced phase separation, for which abundant literature is already available (29). Although necessarily limited and biased by our personal interests, we hope that our overview will help to identify general principles, promising routes and applications of LLCPS for the broader scientific community.

2. Different types of liquid-liquid crystal phase separations

In this section we briefly introduce the three types of LLCPS, occurring when at least one of the components in solution (molecule, polymer or colloid) is prone to LC ordering, *LC forming component*, Fig. 1a. There are two main classes of lyotropic LC forming components: i) *rod-like* components, which have enough stiffness and shape anysotropy to form LC phases, as predicted by Onsager's theory (20) and its extensions, such as long double-stranded DNA (l-dsDNA) > 50 base pairs (bp), filamentous viruses, CNCs (11); or ii) *self-assembling* components, which can form physical linear aggregates in turn ordering in LC phases. This latter case is usually named *chromonic LC ordering* from the partially soluble, disk-like dye molecules which aggregate through $\pi - \pi$ stacking of their aromatic cores (30), but is also observed for short double-stranded DNA oligomers (s-dsDNA) < $20bp$ (31; 32) and single nucleotides (33), amyloid fibers and of course amphiphilic surfactant molecules (24).

Phase separation in simple solutions of a LC forming component is predicted, on a purely entropic basis, as a function of its concentration, C_1 (20) (Fig. 1b). Indeed, at low C_1 the system is in a one-phase ISO liquid, Fig.1.b, while above a threshold concentration, C^*_{ISO}, LC droplets appear in coexistence with ISO. Nematic (N) *tactoids* are perhaps the best known example, with uniaxial orientational order (34; 25; 35; 36). In self-assembling systems, LC domains contain concentrated, longer aggregates than the coexising ISO phase (37). Broader coexistence regions can be found in this case because of the intrinsic polydispersity of aggregating systems (38).

We mostly focus here on LLCPS in multi-component mixtures, where phase separation is driven in an otherwise homogeneous solution of the first component by the presence of a second, *Non-LC forming component*. The latter is not necessarily prone to LC ordering and mainly belongs to the class of flexible polymers, such as single-stranded DNA (ssDNA), PEG, Dextran, peptides or polycations.

Mixing incompatible (repulsive or simply non-interacting) species can lead to the so-called segregative phase separation, in which a component 1-rich phase coexist with a component 2-rich phase in thermodynamic equilibrium (1). In the presence of a LC-forming component, the ordered phase can naturally emerge if the concentration exceeds the transition threshold (Fig. 1c). In an equivalent description, if rod-like molecules are mixed with flexible polymers, the entropic gain from the alignment of rod-like particles and the osmotic pressure from the flexible polymers can combine to drive demixing (13). In the following sections we'll see several examples of this process, also for self-assembling molecules.

Finally, coexistence of two liquid phases can also occur in the case of attractive interactions between the two components (compatible, or adsorbing polymers (1)), as modeled by Flory-Huggins theory (39; 40) Such a situation is typically called associative LLPS, or complex coacervation (10). In mixtures of oppositely charged polyelectrolytes, it is driven by electrostatic attraction and entropic gain of releasing counterions, resulting in a dense phase enriched in both polymeric species and a dilute supernatant phase with the remaining low-valency ions (27; 41) (Fig. 1d). The fact that complex coacervates are usually depicted as disordered bundles of flexible polyions may induce to think that they are incompatible with more ordered states, such as LC, and that in presence of stiff components the only possibility is the transition to solid-like precipitates (42)* and amorphous arrested phases (6; 8; 19). In reality, the dense coacervate phase can be considered as a semidilute polymer solution (43). Since concentrated solutions of semiflexible polymers can display LC ordering (21), it's conceivable that LC phases can arise inside coacervates if one of the polyions has sufficient stiffness (44).

3. Segregative DNA

Phenomena related to DNA conformations and phase behaviour, either as a single polymer or in solution, have been studied since decades. The term "condensation" has been frequently used for both collapse and phase separation, induced by both neutral polymers (the so-called psi-condensation) (47) and multivalent cations (48). Neutral, non-adsorbing polymers like PEG or Dextran have long been used to tune the osmotic pressure in DNA solutions. Their effect can be described in terms of entropic, depletion-type forces due to the difference in flexibility between the two species. At low polymer concentrations, the mixture is typically in a single homogeneous phase and a semipermeable membrane is used to control osmotic pressure, while at higher concentrations phase separation occurs between a polymer-rich and a DNA-rich phase. Increased DNA concentration can in turn promote LC ordering in the case of long, rigid, double-stranded helices (49). The inter-helix distance has been systematically measured - through X-ray diffraction - as a function of osmotic pressure, to extract the equation of state and concentration discontinuities across the transition between isotropic, chiral nematic (N^*) and higher order liquid crystalline phases. Osmotic pressure can be finely tuned also through temperature in the $15 - 45°C$ range, for which DNA-DNA interactions have no detectable changes (50).

Polymer-induced phase separation and LC ordering have been widely investigated for DNA helices above $100bp$ and explained within the context of Onsager's theory for isotropic-nematic transition. More recently, it has been reported that PEG can induce phase separation even in the case of DNA oligomers, both single and double strands (51). At high enough concentration, also double strands as short as $4bp$ can display LC ordering, via the formation of linear, reversible aggregates

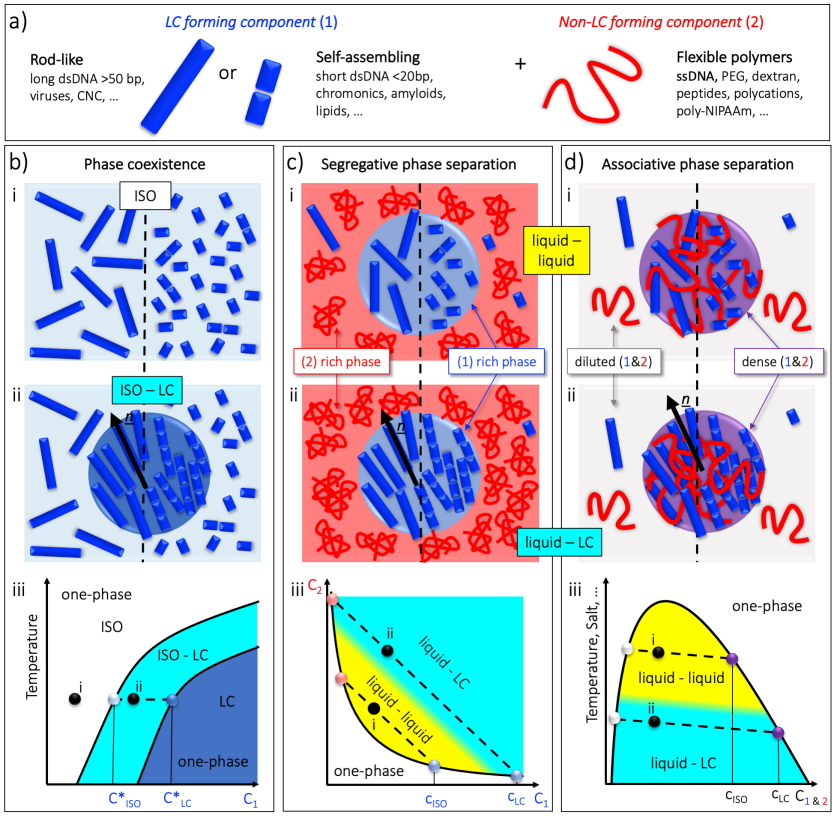

Figure 1: Types of liquid-liquid crystalline phase separations. (a) Sketches and examples of LC forming components (1), either anisotropic *rod-like* particles or *self-assembling* systems, and non-LC forming components (2), such as flexible polymers. (b) Phase separation in solutions of only one LC forming component (i) can take place on a purely entropic basis, between liquid crystal (LC) microdroplets which coexist with a liquid isotropic (ISO) phase (ii). In a typical concentration-temperature ($C_1 - T$) phase diagram of a lyotropic LC system (iii), for a given T, at low C_1 the system is one-phase ISO, while above a threshold concentration, C^*_{ISO}, ISO-LC coexistence takes place in the concentration interval $C^*_{ISO} < C_1 < C^*_{LC}$, above which the system is one-phase LC. Solid black curves are the boundaries between ISO and LC phases. (c) Segregative phase separation in a mixture of incompatible components can lead to the coexistence of a component-1 rich phase, in which transition from ISO (i) to LC (ii) can take place, and a component-2 rich phase. A typical $C_1 - C_2$ phase diagram (iii) shows a binodal curve (black line) above which the system is two-phase. ISO-LC phase transition in component-1 rich phase is mainly driven by the local increase of C_1. (d) Associative phase separation in a mixture of compatible components can lead to a dense coacervate phase, enriched in both component 1 and 2, where transition from ISO (i) to LC (ii) can take place, in coexistence with a diluted supernatant phase. The phase diagram (iii) for a charge-balanced mixture as a function of the attractive interactions (modulated e.g. by T or ionic strength) shows a bell-shaped binodal curve (black line), typical of critical systems, below which the system is two-phase. In (b), (c), (d) the left side refers to rod-like particles and the right side to self-assembling systems. In phase diagrams, black dots are examples of realization of phases sketched in the corresponding i and ii panels, colored dots indicate the composition of the coexisting phases, dashed lines are the tie-lines. In both segregative and associative phase separations, initial global C_1 can be much lower than the required C^*_{LC} for the ISO-LC transition in a one component system.

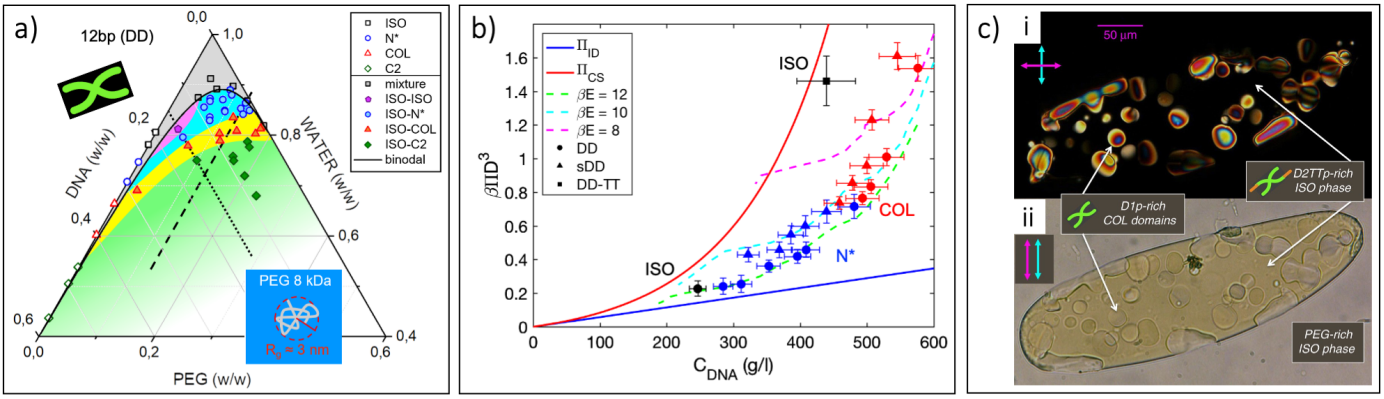

Figure 2: Segregative DNA LLCPS. (a) Ternary phase diagram of aqueous solutions of $12bp$ dsDNA and $8kDa$ PEG. Symbols indicate the initial preparation and the type of observed phase separation. Solid black line is the binodal line, separating the one-phase region (grey shading) and the phase-separation region. Lines indicate constant DNA (dotted) and PEG (dashed) preparations. (b) Comparison of the experimental equation of state, obtained for phase-separated LC-forming (dots, triangles) and non-LC forming (squares) s-dsDNA with PEG, with the prediction of the simulation for a system of sticky cylinders and Carnahan–Starling equation of state for hard spheres (solid red line) and ideal gas equation (blue line). DNA concentration and pressure are estimated from the DNA-rich and PEG-rich phases, respectively. Adapted with permission from ref. (45)*. (c) Optical microscopy images of a three-phase segregative phase separation in a mixture of PEG and LC-forming (D1p) and non-LC-forming (D2TTp) s-dsDNA, obtained with crossed (i) and parallel polarizers (ii). The coexisting phases are: DNA COL domains (coloured domains), DNA ISO phase (black in (i) and pale yellow in (ii)) and PEG-rich ISO phase background (grey in (ii)). Reproduced from ref. (46) under Creative Commons agreement.

(31; 52; 32). Such end-to-end aggregation can occur either through stacking of blunt-end duplexes or through pairing - and stacking - of complementary dangling ends, while it is impaired in the case of non-complementary tails, which in turn suppresses LC ordering. PEG-induced phase separation and mesoscopic ordering of DNA duplexes with different terminal motifs have been extensively investigated in (45)*. Fig. 2a reports the ternary phase diagram and the observed LC phases for a blunt-end dodecamer. At constant PEG concentration, phase separation is found above a threshold DNA concentration, which decreases for increasing PEG. At high PEG, only highly ordered DNA phases are observed. The phase separation boundaries for aggregation-prone DNA and PEG and the degree of partitioning of the species in the coexisting phases allows to determine the experimental equation of state. This significantly departs from the classical Carnahan-Starling equation for hard spheres, except for ISO-ISO demixing (see Fig. 2b). Instead, it is found to be in agreement with computer simulations on aggregating cylinders (53), which accounts for the end-to-end attractive interactions and the more effective packing within LC phases. The effect of ionic strength remains to be studied in detail.

Strikingly, spontaneous demixing has been observed also in the case of solutions containing only DNA strands, if their sequences allowed the formation of a population of duplexes in coexistence with single strands (31; 52). In this DNA-only system, the osmotic pressure from the single strands is able to trigger phase separation only when double strands can also display LC ordering, through linear aggregation; on the other hand, the overall concentration of duplexes alone would be insufficient to drive LC ordering without the additional contribution from single strands, nested in their very different flexibility. This intriguing coupling suggests that the free energy gain associated with end-to-end aggregation and LC ordering is critical in driving the phase separation and bears important implications. In a system of random sequences, which can form a wide spectrum of partially- and fully-paired structures, duplexes capable of stacking and/or pairing can spontaneously demix, upon LC ordering, from the multitude of duplexes with structures incapable of aggregation, and thus of LC ordering, which stay in the ISO phase (54). Moreover, mixtures of PEG and duplexes capable and incapable of aggregation can undergo multiple phase separations, with DNA-rich droplets further demixing into LC domains and an isotropic fluid mainly composed by non-aggregating strands (46) (Fig. 2c). Besides a simple mechanism of compartmentalization (55), the selectivity of this cascaded phase separation of sequences provides a self-sorting mechanism for complementary sequences and stable structures with sufficiently adhesive terminals. This may have constituted a selection principle, a template and an efficient pathway for the emergence of linear nucleic acids polymers in a prebiotic environment, within the so-called RNA world. This hypothesis has been tested by investigating the non-enzymatic ligation of RNA oligomers (56)**. It has been found that in presence of demixing, self-assembly and LC ordering the ligation yield is greatly enhanced over homogeneous or isotropic solutions, as estimated from gel electrophoresis. The linear aggregates favour intermolecular reactions over intramolecular ones, and the increased local concentration in LC domains boosts the ligation rate.

4. Associative DNA

As mentioned above, condensation of long dsDNA by multivalent cations, such as polyamine (putrescine^{2+}, spermidine^{3+}, spermine^{4+}, hexammine cobalt^{3+}), has been widely explored in the past decades as a method to produce the collapse of long DNA chains (e.g., lambda phage DNA $\sim$ $50kbp$) into hexag-

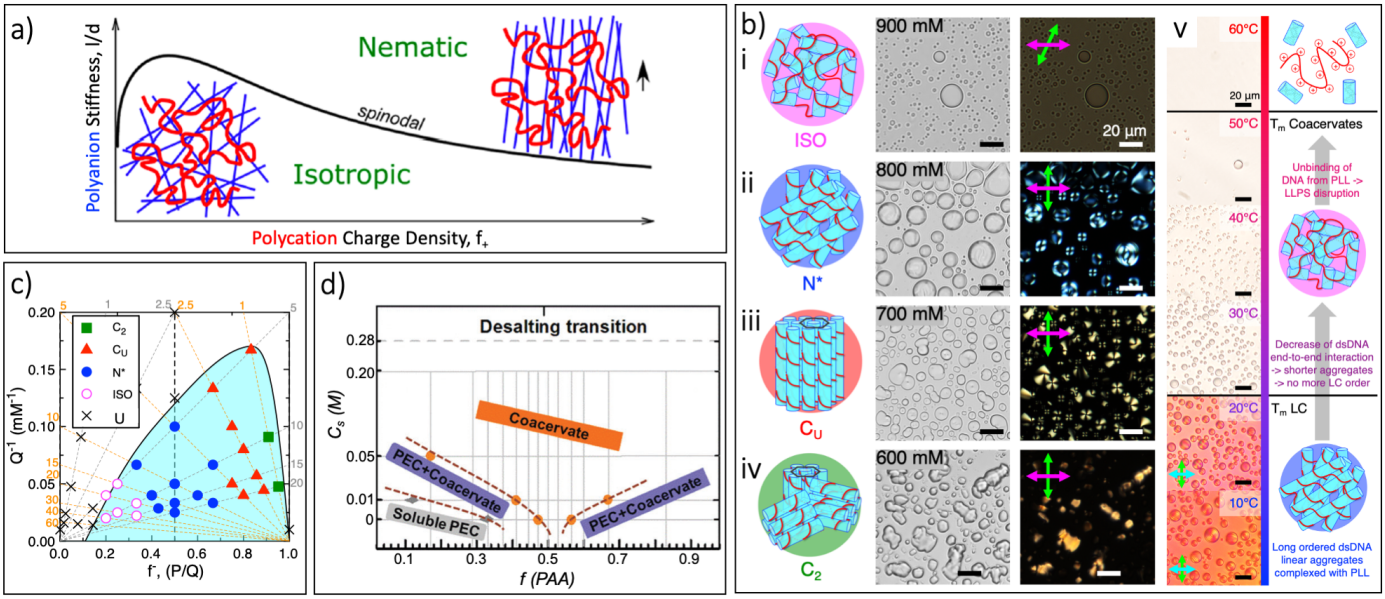

Figure 3: Associative DNA LLCPS. (a) Schematic spinodal with respect to nematic ordering as a function of polycation charge density, f_+, and polyanion stiffness, V_d. Representation of stiff polyanions (blue) and flexible polycations (red) in nematic and isotropic dense coacervate phase. (b) Schematic representation and optical microscopy images, without and with crossed polarizers, of LC complex coacervates composed by 12mer dsDNA and poly-lysine, displaying ISO (i), chiral nematic N^* (ii), columnar uniaxial C_U (iii), and columnar crystalline C_2 (iv) phases at decreasing NaCl concentrations. Transitions from N^* to ISO coacervates, to homogeneous phase, driven by the destabilization of DNA-DNA stacking and DNA-PLL electrostatic interactions at increasing temperature (v). (c) Phase diagram of charge-unbalanced solutions of s-dsDNA and PLL, as a function of the fraction of negative DNA charges, f^-, and the inverse of the total charge, Q^{-1}, at constant 800mM NaCl. Dashed gray and orange lines represent constant negative DNA and positive PLL charge concentration, respectively. Symbols indicate the observed coacervate phase, showing the prevalence for N^* phase close to charge balance, ISO phase at low f^-, i.e. excess of PLL, and COL phase at high f^-, excess of DNA. (d) Phase diagram of early stage kinetic behavior in the formation of PAA/PDADMAC complexes as a function of the ionic strength C_S and the mixing ratio of PAA, $f(PAA)$ obtained from stopped-flow light scattering measurements. Reproduced with permission from refs. (44), (57), (58)**, (59), respectively.

onally packed structures named *toroids* (60; 48). Polyamine-induced precipitation of moderately long dsDNA (146bp) can promote the formation of chiral nematic and hexagonal LC phases (61; 62). Through X-ray diffraction it has been shown that the transition between the different phases and the corresponding variation of the inter-helical spacing are strongly affected by ionic strength and polyamine type (63). Similar results are found with shorter dsDNA (25bp) condensed by spermidine and spermine (64), although the phase state within the precipitates was not clear. The scientific community is more and more turning its attention to complex coacervation as a proxy for the behaviour of intracellular membraneless organelles (6), with nucleic acids and cations and/or intrinsically disorded proteins (65). The phases formed by complexation of DNA oligomers and disordered cationic peptides have been systematically investigated, as a function of total concentration, polymer length (10 to 88 nt DNA sequences, 10 to 100 amino acids poly-Lysine, PLL) and charge ratio (42)*. Remarkably, coacervation strongly depends on nucleic acids hybridization: while ssDNA yields liquid droplets, dsDNA mainly produces solid precipitates, which has been proposed to result from the larger charge density of dsDNA over ssDNA. Transition from precipitates to liquid droplets can be obtained by increasing ionic strength or temperature, which lowers the electrostatic interactions between the polyelectrolytes. Also dsDNA flexibility plays a crucial role in the phase behaviour. Investigation of mixtures of PLL and different ssDNA and dsDNA oligomers has shown that GC-containing sequences, more flexible than AT-rich sequences, require less salt to form droplets, indicating that even a small difference in persistence length can have major effect on LLPS (66)**. Surprisingly, at high salt concentration both 22mer poly(GC) and poly(AT) dsDNA form chiral nematic LC phases, a result of the high local concentration in the droplets and possibly of linear aggregation of ds-DNA. Moreover, if half of the negative charges are replaced by nucleotides triphosphates (NTPs), at fixed ionic strength precipitates are replaced by droplets. Interestingly, such PLL-dsDNA-NTP droplets further demix into LC domains, whose textures recall highly ordered columnar phases often observed for s-dsDNA LC (31; 32), and an isotropic phase rich in NTPs. An elegant theory of coacervation in mixtures of rigid polyanions (such as dsDNA) and flexible polycations (such as PLL or other petides) has been recently proposed (44). Based on scaling approach and random phase approximation, this theoretical framework predicts a transition from isotropic coacervates to LC ones as the polyanion stiffness exceeds a threshold value (Fig. 3a). In such conditions, as in a bulk lyotropic system, the transition to the nematic phase is driven by the anisotropic interactions (excluded volume and electrostatics) between the stiff polyanions.

An even richer behaviour has been reported for mixtures of dsDNA 12mers and PLL, in which phase separated microdroplets display all known mesophases for the pure s-dsDNA at high concentration (58)**: ISO, chiral nematic (N^*), uniaxial

columnar (C_U) and high order columnar (C_2) (Fig. 3b). The LC coacervate phases result from the supramolecular assembly of DNA duplexes complexed with the polypeptide; indeed, the suppression of end-to-end DNA aggregates, either by temperature or with specific sequences, causes the disappearance of LC phases, which are replaced by conventional ISO coacervate microdroplets (57). Variations in ionic strength and DNA concentration, as well as peptide concentration and stoichiometric ratio (Fig. 3c), all tune the phase boundaries with continuity. Remarkably and counterintuitively, this system can escape precipitation simply by drying, and accesses ordered, yet fluid, phases by dilution. The internal structure of the LC coacervates is reconstructed from the quantitative knowledge of bulk DNA mesophses and of l-dsDNA-polyamine condensed phases (63). It leads to an estimated DNA local concentration, inside LC droplets, between 100 and 1000 times the starting average concentration. As mentioned in Section 4, LLCPS may also have played a role in the prebiotic emergence of nucleic acid linear polymers in prebiotic environment. In this perspective, the concentration boost enabled by LLCPS is even more remarkable, as it provides a formidable spontaneous compartmentalization mechanism.

4.1. Pathway to DNA LC coacervates

From the observations above, an open question arises: is LC formation a consequence of LLPS, or is it caused by the rearrangement of precipitate precursors (i.e., a liquid-solid phase transition)? The possible answer is related to the kinetics of coacervation in mixtures of oppositely charged polyeletrolytes - a debated topic in literature - and depends on different factors, such as polymer chain length, charge pattern and symmetry, added salt, pH (67) and the experimental mixing procedure (68). Stopped-flow light scattering experiments have evidenced different early stage kinetic behaviors in the formation of polyelectrolyte complexes (PECs), depending of charge ratios (59): full coacervation is favored at charge neutrality and/or at high ionic strength, while far from charge neutrality aggregation and/or rearrangement of small soluble PECs into larger structures prevail (Fig. 4d). In the case of the assembly of LC-coacervates in mixtures of short dsDNA and PLL (58), it's possible to envision a similar scenario (Fig. 3b,c): columnar phases, found at lower ionic strength and/or in asymmetric (DNA rich) mixtures, only appear after thermal annealing, which suggests rearrangement of out-of-equilibrium precipitates; on the contrary, ISO and N^* coacervates, appearing at low temperature, at high ionic strength and/or close to charge neutrality, are likely equilibrium states mainly arising from liquid-liquid phase separation.

4.2. Segregative and *associative phase separation*

A unified experimental approach to associative and segregative phase separation has been recently proposed (69)*. The phase behaviour of DNA strands between $12bp$ and $50kbp$ is investigated upon the addition of either PEG and Mg^{2+} ions (Polymer- and Salt-Induced, PSI, condensation), or the Histone linker protein (H1 condensation). In both cases, the condensing agents trigger compaction of dilute DNA molecules and, above a critical DNA concentration, phase separation of a DNA-dense phase. The morphology and viscoelastic properties of the condensed domains are investigated through microscopy and FRAP measurements, to quantify their internal mobility. While short DNA strands typically form spherical, liquid-like droplets, longer strands preferentially condense into irregular and less dynamic assemblies, with a transition length between $1k$ and $10kbp$ in both segregative and associative phase separation. Interestingly, a similar effect is found also in fragments of reconstituted chromatin, whose degree of compaction in the cell nucleus affects and modulates transcription efficiency. Titration experiments with histone H1 proteins also suggest that the degree of fluidity inside the phase-separated domains is determined by the number of attractive interactions. Since for some lengths we already know that in between liquid and solid droplets, LC ordering emerges (51; 61; 58)**, it would certainly be useful to systematically further investigate the local concentration and the degree of alignment of the DNA strands inside such droplets within the transition region.

5. Other systems

In several other systems, either self-assembling, like chromonics, or structurally rod-like, like viruses, we can observe a rich interplay between liquid crystalline ordering and phase separation phenomena, both segregative and associative. We discuss here few selected examples which well represent the common features, some peculiarities and relevant open questions in the field.

5.1. Chromonics

Chromonics are a prototypical class of materials whose LC ordering is intrinsically nested in their self-assembly: they are flat, rigid molecules composed of aromatic rings with peripheral charged hydrophilic groups, forming reversible linear aggregates in water, which in turn can align in nematic (N) and columnar (C) mesophases (30). They include drugs like cromolyn (DSCG), dyes like Sunset Yellow (SSY) and nucleotides (33), with the aggregating DNA oligomers mentioned in section 3 sharing some features.

Their phase behaviour can be strongly affected by the presence of ions or co-solutes. Early investigations (72) reported that several water-soluble, nonionic polymers like polyvinyl alcohol can induce phase separation, and LC ordering within the condensed phase, at concentrations below the ISO-N transition for pure systems. The chemical features of the polymers determine the emergence, stability and configuration of the LC droplets. Interestingly, PEG does not induce phase separation in isotropic DSCG solutions, but, when added to a homogeneous nematic phase, it increases the temperature for N-ISO transition (73). However, it also widens the coexistence region and recent microscopy and X-ray diffraction measurements showed that the phase separated LC domains are in the columnar phase (74). In isotropic SSY solutions, PEG can trigger the elongation of aggregates and the phase separation between a LC phase and an isotropic PEG-rich phase; when added to homogeneous

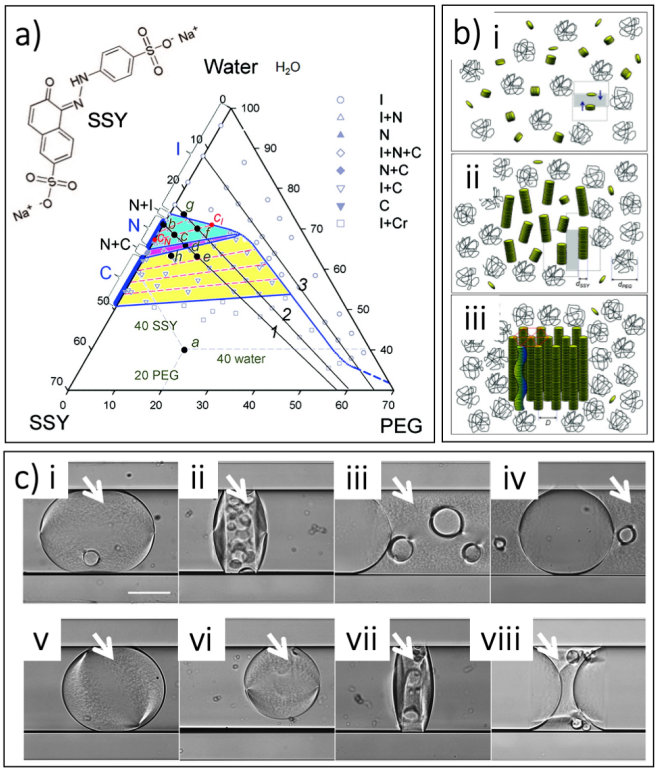

Figure 4: LLCPS in chromonics (a) Ternary phase diagram of Sunset Yellow and PEG water mixtures in the ISO, N and C phases and their coexistence. (b) Sketches of the excluded volume effect at increasing PEG concentration on chromonic assembly: short aggregates assembly (i), parallel ordering of longer aggregates in the N phase (ii) and hexagonal ordering of very long aggregates in the C phase (iii). Reproduced with permission from ref. (70)*. (c) Effects of molecular weight and concentration of PEG on the wetting behavior of the ISO and N coexisting phases of 26.0% (wt/wt) SSY, confined in a 200 μm capillary. Short white arrows indicate nematic regions. (i–iii) SSY with 0.01% (wt/wt) PEG with molecular weight of 35, 1, and 0.4 kDa, respectively. (iv) SSY with no PEG. (v–viii) SSY with 0.1, 0.01, 0.001, 0.0001% (wt/wt) of 8k PEG, respectively. Reproduced from ref. (71) with permission from The Royal Society of Chemistry.

N and C phases, it leads to coexisting ISO-N and ISO-C phases, respectively (70)*. Fig. 4a displays a ternary diagram for this system and sketches of the mixed and demixed phases. Such behaviour is tuned by ionic strength, which acts on aggregate length and flexibility. Recently, it was shown that even at extremely low concentrations, well below the phase separation threshold, PEG can dramatically change the wetting behaviour of the N phase of SSY from low to high contact angles, likely because of adsorption to the substrate (71) (Fig. 4b). A very rich phase behaviour can emerge when two chromonic species are mixed, with various single- and two-phase regions (75). Some studies have also addressed associative phase separation and the effect of solvent properties in chromonics. Overall, multivalent ions like spermine destabilize the N phase, lowering the N-ISO temperature and triggering separation between ISO and N/C domains (76; 73). Intriguing differences emerge between added spermine salt or the free base, likely related to pH effects. However, the phase diagram of SSY is only slightly affected by the addition of polar solvents like urea and formamide (77). Overall, a delicate balance emerges and the role of hydration and competing effects at the various stages of self-assembly remains to be fully investigated and understood.

A particular class of chromonics is constituted by DNA nucleotides. In particular, the DNA nucleoside Guanosine (G), with one (GMP) or three (GTP) phosphate groups, can form quartets via non-canonical hydrogen bonds. It is known that multiple G-quartets, stabilized by stacking interactions, can form within G-rich DNA strands via intra-chain folding. The conformational transition to this ordered structure, which plays a biological role e.g. in telomeres, is stabilized by PEG and monovalent and multivalent ions (78; 79). Moreover, in the presence of Histone linker protein H1, G-rich DNA strands undergo LLPS more easily than sequences unable to fold in quadruplexes, showing that a critical balance of charge density, rigidity and stacking interactions is at play (80). Back to the more chromonic-like GMP single nucleotides, stacks of G-quartets can form four-stranded helices in solution which in turn, at high enough concentration, order into N^* and C phases. The addition of PEG favours their phase separation and LC ordering (81). The importance of stacking in tuning the phase behaviour once again emerges in mixtures of single nucleotides and polypeptides (82)*. All nucleotides form coacervates below specific temperature and ionic strength values, but LLPS propensity and partitioning are stronger for purines (GTP and ATP), in agreement with their larger stacking free energy.

5.2. Nanocellulose

Cellulose, one the most abundant biopolymers on Earth, can be extracted in various hydrophilic forms, including long microfibrils and rod-like nanocrystals (86). The latter can display chiral nematic LC ordering, which makes them appealing for applications, like the realization of thin films with photonic properties. However, spontaneous LC ordering in elongated CNCs often competes and overlaps with the formation of arrested phases, gels and glasses depending on the balance between attractive and repulsive interactions (87; 83) (Fig.5a). Indeed, the typical concentrations for ISO-N transition, caging

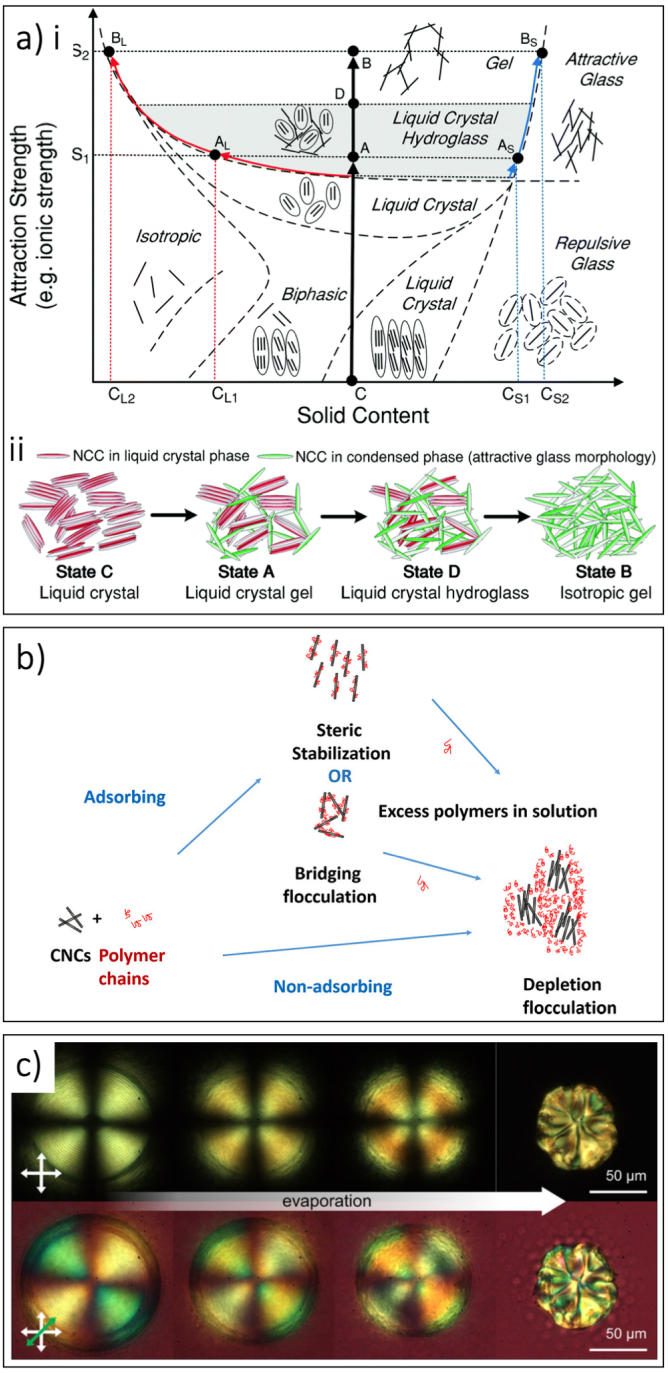

Figure 5: LLCPS in nanocellulose systems (a) Schematic phase diagram (i) and phase transitions (ii) for the formation of liquid crystal "hydroglass" by spinodal decomposition in nanocellulose suspensions, proposed from experimental phase boundaries and rheological characterization. (b) Schematic illustration of how neutral and negatively charged polymers are thought to affect the behaviour of rod-shaped CNCs. (c) Experimental observation of the evolution of chiral nematic textures for water-in-oil droplet-confined CNCs, crossed polarizers (top row) or upon addition of a retardation plate (bottom row). Over time, water partially mixes with the surrounding hexadecane oil, increasing CNC concentration and inducing eventual drying of the droplet (from left to right). Reproduced with permission from refs. (83), (84) and (85), respectively

or percolation, all scale with the effective aspect ratio of the nanocrystals (12). For these reasons, the conditions affecting the phase behavior of CNCs, including ionic strength (83), length (88) and solvent properties (89; 90), have been extensively investigated. Often, the overall interaction balance leads to partial phase separation, with LC domains jammed in a random network (90). Seminal studies with high molecular weight Dextran found that the addition of the polymer to N samples triggers phase separation and high degree of partitioning, but it cannot induce demixing in isotropic solutions (91). Microscopy observations and rheological measurements highlight important differences between the neutral PEG and a polyelectrolyte (carboxymethyl cellulose) added to the negatively charged CNCs (92; 84): the charged polymer favors aggregation and phase separation of a LC, CNCs-rich phase in a wide range of concentrations, while the neutral polymer partially coats the nanocrystals and stabilizes them, only inducing weaker depletion interactions, unable to trigger phase separation (Fig. 5b). The investigation has been extended to polymers with various charge and structural properties (93)*. The addition of positively-charged polymers result in strong enhancement of the measured viscoelastic moduli through bridging, but in some instances phase separation is arrested. The overall emerging picture suggests that the occurrence of segregative and/or associative phase separation is finely tuned by the detailed balance of interactions and steric properties of the components. Finally, we mention an interesting strategy exploited in both chromonics (94) and nanocellulose (85) to explore concentration and confinement effects in water-in-oil droplets. The partial solubility of water in hexadecane leads to progressive evaporation, in turn causing shrinkage and texture evolution until complete drying (Fig. 5c). Interestingly, such method captures a change in the concentration scaling of the chiral nematic pitch, corresponding to the kinetic arrest and consequent hindering of stress relaxation.

5.3. Actin

Phase behavior and alignment within actin networks, a major constituent of the cytoskeleton, play a central role in their mechanical properties and the cellular machinery (98; 99). Homogeneous solutions of actin filaments undergo transition to nematic ordering at sufficiently high concentrations (35). Interestingly, short filaments display a first order transition and nucleation of nematic tactoids with higher concentration and degree of ordering than the surrounding isotropic solution (Fig. 6a.i), while longer filaments show a continuous phase transition with no demixing (35). Like in other systems described in this review, it is observed that a similar phase separation of nematic domains can be triggered at much lower concentrations by the addition of a cross-linking species, like the filamin protein, which favors alignment of actin within the fluid droplets (95)** (Fig. 6a.ii). Surprisingly, however, higher filamin concentration yields less elongated tactoids, because this long and flexible cross-linker effectively acts as an isotropic surface tension, increasing internal cohesion and overcoming filament alignment. Longer filaments and high cross-linking density eventually lead to the formation of viscoelastic networks. It

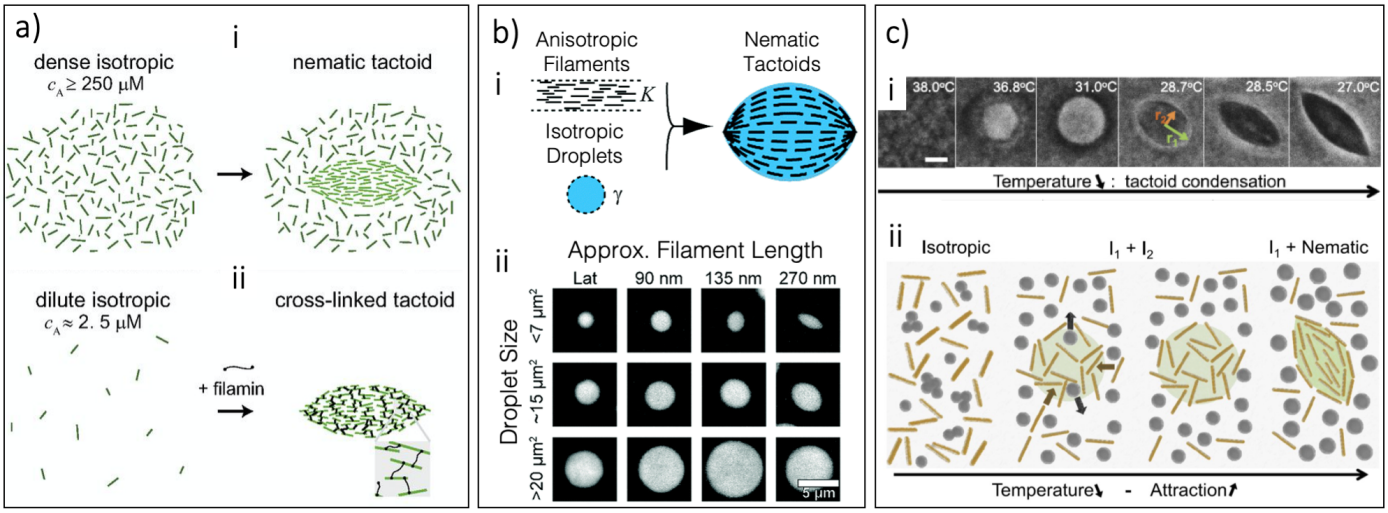

Figure 6: LLCPS in actin and virus systems (a) Liquid crystal droplets of F-actin. Tactoids formation near the (concentration-driven) isotropic–nematic phase transition (i) and induced by the addition of cross-linkers (ii). (b) Schematics of the transition from circular isotropic droplets to bipolar nematic tactoids, induced by the addition of actin filaments, contributing a nematic elastic energy, to FUS droplets, providing an isotropic interfacial energy (i). Fluorescence micrographs of FUS droplets for increasing actin filament length and droplet size (ii). The addition of latrunculin (Lat), which prevents actin polymerization, yields spherical droplets. (c) Condensation of nematic tactoids as a function of temperature, in a colloidal suspension of M13K07 viruses and poly-NIPAAm microgel particles, imaged by phase contrast microscopy (i). Schematic interpretation of the tactoid condensation (ii). As temperature is lowered, poly-NIPAAm particles swell causing depletion-like attraction between virus particles. In the ISO-ISO coexistence, rods are concentrated in the droplet and microgel particles are expelled, leading to ISO-N transition. Reproduced with permission from refs. (95)**, (96) and (97)*, respectively

is tempting to look for similar effects in DNA filaments of different length. Actin can act in a somehow complementary role when it is added as anisotropic dopant in fluid droplets (Fig. 6b.i) (96). FUS is an RNA-binding protein which phase separates in liquid droplets at sufficiently low ionic strengths. By adding actin, composite droplets are formed, whose viscosity and anisotropy increase with the concentration and length of actin, which imparts LC ordering to the system (Fig. 6b.ii) (96). The overall shape of the droplets can be understood in terms of the balance between the surface tension and an average nematic elastic constant.

5.4. Viruses

Filamentous viruses are natural, monodisperse, rod-like colloids with high aspect ratio (few nanometers in diameters and micrometer-scale length) and their LC ordering shares several common features with other stiff, elongated biomacromolecules like CNCs, amyoloid fibers (11) or DNA-based rods (100). Polymers have long been used to tune the phase behavior of viruses, providing an extremely rich playground to test LC theories about the role of flexibility and interactions on transition concentrations and order parameters (101). They can also promote the formation of 2D, smectic membranes, where the interplay between molecular chirality and surface tension (effectively controlled by the polymer-controlled depletion interaction) can give rise to reconfigurable structures like twisted ribbons (102). If the viruses are mixed with poly-NIPAAm microgels, fine tuning of interactions is made easier as their volume is strongly dependent on temperature (97)*. Phase separation into nematic tactoids is mediated by the prior formation of isotropic, concentrated droplets of viruses in coexistence with microgel-rich background (Fig. 6c).

6. Conclusions and perspectives

We have presented the basic principles of liquid-liquid crystal phase separation and reported examples for several different biomolecular systems. Addition of effective attractive interactions to a LC-prone system often results into LLCPS, either associative or segregative.

6.1. What does LLPS bring to LCs?

LC ordering can be affected by LLPS in at least two ways: *(i)* the total concentration for ISO-LC phase transitions is lowered (Fig. 1) by as much as 2-3 orders of magnitude (57); *(ii)* the LC phase diagram can be finely tuned by the physicochemical properties of the second component, which are often easier to control (such as in the case of PEG or poly-NIPAAm). This aspect is particularly relevant for the self-assembly of aggregating systems, such as chromonics. Phase separation has been extensively exploited in the context of thermotropic LCs, finding numerous applications in material science, for tuning crystallinity and molecular packing at nano/macroscopic length scales (103), for realizing polymer-dispersed LCs (29) and for polymer-stabilized LCs for photonics. (104). A similar approach is increasingly applied to lyotropic LCs (105), whose optical (86; 106) and viscoelastic properties (96; 107) can prove beneficial for technological advances in the photonic and biomaterial fields.

6.2. What does LC ordering bring to LLPS?

LC ordering can result in enhanced funcionalities, in particular in biomolecular systems. For example, as discussed in section 5.3, doping an isotropic LLPS with an anisotropic component can induce N ordering and novel mechanical

properties (Fig. 6). LLCPS can also act as permeable microreactors regulating and enhancing chemical reactions involving nucleic acids (46; 56)**. We can further envision multiphase complex coacervates (108) exhibiting an internal ISO-N phase separation (66; 58) as tools to control spatial organization, reaction yield and responsiveness to stimuli (temperature, light, mechanical stress) in synthetic compartments. The propensity of DNA and RNA molecules to produce such phases could integrate the use of recently developed enzyme-bases DNA-toolboxes and DNA nanotechnology methods (109). Finally, the role of LLPS in cellular organization (5) could gain an extra twist from theoretical tools and formalism developed for LCs. Examples range from time evolution (maturation) in intracellular membraneless organelles (6) to organization of genomic DNA (110) to amyloids. The latter are fibrillar protein aggregates which form LC phases *in vitro* (111; 112)*, undergo phase transition to arrested states *in vivo* (113; 114) and display intriguing evolution from bundles to fibers and other aggregates upon complexation with intrinsically disordered proteins (115).

We hope that this review will stimulate the reader to further probe the intimate connection between liquid crystals and the biological world, and to investigation new and diverse LLCPS systems.

Acknowledgements

We wish to thank all the colleagues involved in the research on DNA liquid crystals over the years, in particular Noel Clark, Tommaso Bellini and Marco Todisco, for inspiring discussions. T.P.F. is supported by a Junior Research Chair fellowship from IPGG (laboratoire d'excellence, "Investissements d'avenir" program ANR-10-IDEX-0001-02 PSL and ANR-10-LABX-31), ANR-10-EQPX-34 and IPGG AAP High Risk 2020 grant.

References

Papers of particular interest, published within the period of review, have been highlighted as:

* of special interest

* * of outstanding interest

(45)* Experimental determination of the PEG/DNA phase diagrams for duplexes having different end-to-end interactions. Detailed description of a simple method for measuring the osmotic pressure and the concentration of LC phases in ATPS.

(56)** Experimental demonstration that PEG induced phase separation and LC ordering both enhance chemical ligation of oligomeric RNA. Remarkably the template effect of the LC phase further boosts reaction kinetics and favors linear products over circular ones.

(42)* Broad experimental investigation of complexation of oligonucleotides with cationic peptides, spanning a wide range of polymer lengths, concentrations and structures. It shows that the phase is controlled by the hybridization state of the nucleic acid: dsDNAs form solid precipitates, while ssDNAs form liquid coacervates, because of their lower charge density.

(66)** First observation of transition from solid precipitates to liquid crystal cholesteric phases in coacervates formed by oligomeric dsDNA and cationic peptides as a function of ionic strength.

(58)** First report and characterization of the various LC mesophases in coacervates formed by oligomeric dsDNA and cationic peptides as a function of ionic strength, temperature, polymer concentration and charge ratio.

(69)* First systematic investigation of the influence of DNA length on the properties of the condensed phase in segregative (PEG) and associative (histone H1) phase separations.

(70)* Multi-technique experimental study of the phase behavior of water solutions of self-assembling chromonic SSY mixed with PEG. Condensation of isotropic SSY solutions into LC phase-separated domains is related the depletion effects acting at the level of aggregate assembly and inter-aggregate ordering.

(82)* Systematic investigation of a wide range of peptidenucleotide coacervates, as a function of temperature and salt concentration, showing the contribution of non-electrostatic base stacking interactions to phases stability.

(93)* Experimental determination of the phase diagrams and rheological behavior of rod-like cellulose nanocrystals incorporated in polymers with different charge and structure.

(95)** Observation of a liquid phase of actin filaments and transition to anisotropic tactoids droplets in the presence a physiological cross-linker, filamin, suggesting a mechanism to control subcellular morphology, organization and dynamics.

(97)* Careful study of the use of poly-NIPAAm microgel particles to induce temperature-dependent depletion attraction between rod–like viruses and first report of ISO-ISO phase separation in this colloidal system.

(112)* First observation of cholesteric phases in amyloids systems composed by -lactoglobulin fibrils under shear stresses, showing transitions, driven by confinement, between at least three types of nematic and cholesteric tactoids.

References

[1] P. Albertsson, Partition of Cell Particles and Macromolecules, 3rd Edition, Wiley, New York, 1986.

[2] M. A. Ghalia, Y. Dahman, Advanced nanobiomaterials in tissue engineering: Synthesis, properties, and applications, in: Nanobiomaterials in Soft Tissue Engineering: Applications of Nanobiomaterials, Elsevier Inc., 2016, pp. 141–172. doi:10.1016/B978-0-323-42865-1.00006-4.

[3] S. Xu, H. Zhang, B. Qiao, Y. Wang, Review of Liquid-Liquid Phase Separation in Crystallization: From Fundamentals to Application (2021). doi:10.1021/acs.cgd.0c01376.

[4] A. V. Ceballos, C. J. McDonald, S. Elbaum-Garfinkle, Methods and Strategies to Quantify Phase Separation of Disordered Proteins, in: Methods in Enzymology, Vol. 611, Academic Press Inc., 2018, pp. 31–50. doi:10.1016/bs.mie.2018.09.037.

[5] A. A. Hyman, C. A. Weber, F. Jülicher, Liquid-liquid phase separation in biology (2014). doi:10.1146/annurev-cellbio-100913-013325.

[6] Y. Shin, C. P. Brangwynne, Liquid phase condensation in cell physiology and disease, Science 357 (6357) (2017). doi:10.1126/science.aaf4382.

[7] I. Peran, T. Mittag, Molecular structure in biomolecular condensates (2 2020). doi:10.1016/j.sbi.2019.09.007.

[8] S. Alberti, D. Dormann, Liquid–Liquid Phase Separation in Disease, Annual Review of Genetics 53 (1) (2019) 171–194. doi:10.1146/annurev-genet-112618-043527.

[9] K. K. Nakashima, M. A. Vibhute, E. Spruijt, Biomolecular chemistry in liquid phase separated compartments, Frontiers in Molecular Biosciences 6 (APR) (2019). doi:10.3389/fmolb.2019.00021.

[10] N. Martin, Dynamic Synthetic Cells Based on Liquid–Liquid Phase Separation (10 2019). doi:10.1002/cbic.201900183.

[11] G. Nyström, R. Mezzenga, Liquid crystalline filamentous biological colloids: Analogies and differences (11 2018). doi:10.1016/j.cocis.2018.08.004.

[12] M. J. Solomon, P. T. Spicer, Microstructural regimes of colloidal rod suspensions, gels, and glasses (2010). doi:10.1039/b918281k.

[13] R. Sear, Phase Behaviour of Athermal Mixtures of Rigid-Rod and Flexible Polymers, Journal de Physique II (6) (1997). doi:10.1051/jp2:1997107{\"{i}}.
URL https://hal.archives-ouvertes.fr/jpa-00248483

[14] Madden, Herzfeld, Liquid crystal phases of self-assembled amphiphilic aggregates, Philosophical Transactions of the Royal Society of London. Series A: Physical and Engineering Sciences 344 (1672) (1993) 357–375. doi:10.1098/rsta.1993.0095.
URL https://royalsocietypublishing.org/doi/abs/10.1098/rsta.1993.0095

[15] O. Annunziata, N. Asherie, A. Lomakin, J. Pande, O. Ogun, G. B. Benedek, Effect of polyethylene glycol on the liquid-liquid phase transition in aqueous protein solutions, Tech. rep.
URL www.pnas.orgcgidoi10.1073pnas.212507199

[16] O. Galkin, P. G. Vekilov, 12 6277-6281 CHEMISTRY Downloaded at BIO-RESEARCH LIB on, Tech. rep. (2000).
URL www.pnas.org

[17] Y. Hata, T. Sawada, T. Serizawa, Macromolecular crowding for materials-directed controlled self-assembly (2018). doi:10.1039/C8TB02201A.

[18] S. Boeynaems, A. S. Holehouse, V. Weinhardt, D. Kovacs, J. Van Lindt, C. Larabell, L. V. D. Bosch, R. Das, P. S. Tompa, R. V. Pappu, A. D. Gitler, Spontaneous driving forces give rise to proteinRNA condensates with coexisting phases and complex material properties, Proceedings of the National Academy of Sciences of the United States of America 116 (16) (2019) 7889–7898. doi:10.1073/pnas.1821038116.

[19] A. Patel, H. O. Lee, L. Jawerth, S. Maharana, M. Jahnel, M. Y. Hein, S. Stoynov, J. Mahamid, S. Saha, T. M. Franzmann, A. Pozniakovski, I. Poser, N. Maghelli, L. A. Royer, M. Weigert, E. W. Myers, S. Grill, D. Drechsel, A. A. Hyman, S. Alberti, A Liquid-to-Solid Phase Transition of the ALS Protein FUS Accelerated by Disease Mutation, Cell 162 (5) (2015) 1066–1077. doi:10.1016/j.cell.2015.07.047.

[20] L. Onsager, The effects of shape on the interaction of colloidal particles, Annals of the New York Academy of Sciences 51 (1949) 627–659.

[21] A. N. Semenov, A. R. Khokhlov, Statistical physics of liquid-crystalline polymers, Soviet Physics Uspekhi 31 (11) (1988) 988–1014. doi:10.1070/pu1988v031n11abeh005643.
URL http://dx.doi.org/10.1070/PU1988v031n11ABEH005643

[22] I. W. Hamley, Liquid crystal phase formation by biopolymers, Soft Matter 6 (9) (2010) 1863–1871. doi:10.1039/b923942a.

[23] J. Zhao, U. Gulan, T. Horie, N. Ohmura, J. Han, C. Yang, J. Kong, S. Wang, B. B. Xu, M. Frenkel-Pinter, M. Samanta, G. Ashkenasy, L. J. Leman, Advances in Biological Liquid Crystals, Small 15 (18) (2019) 1900019. doi:10.1002/smll.201900019.
URL https://doi.org/10.1002/smll.201900019

[24] G. T. Stewart, Liquid crystals in biology I. Historical, biological and medical aspects, Liquid Crystals 30 (5) (2003) 541–557. doi:10.1080/0267829031000097457.
URL http://www.tandfonline.com/doi/abs/10.1080/0267829031000097457

[25] P. Azzari, M. Bagnani, R. Mezzenga, Liquid-Liquid Crystalline Phase Separation in Biological Filamentous Colloids: Nucleation, Growth and Order-Order Transitions of Cholesteric Tactoids, Soft Matter (2021). doi:10.1039/D1SM00466B.
URL http://pubs.rsc.org/en/Content/ArticleLanding/2021/SM/D1SM00466B

[26] E. Albertsson, PARTITION OF CELL PARTICLES AND MACRcOMOLECULES IN POLYMER TWO-PHASE SYSTEMS, Tech. rep.

[27] J. v. d. Gucht, E. Spruijt, M. Lemmers, M. A. Cohen Stuart, Polyelectrolyte complexes: Bulk phases and colloidal systems, Journal of Colloid and Interface Science 361 (2) (2011) 407–422. doi:10.1016/j.jcis.2011.05.080.

[28] J. T. King, A. Shakya, Phase separation of DNA: From past to present (4 2021). doi:10.1016/j.bpj.2021.01.033.

[29] M. H. Saeed, S. Zhang, Y. Cao, L. Zhou, J. Hu, I. Muhammad, J. Xiao, L. Zhang, H. Yang, Recent Advances in The Polymer Dispersed Liquid Crystal Composite and Its Applications (11 2020). doi:10.3390/molecules25235510.

[30] J. Lydon, Chromonic review (12 2010). doi:10.1039/b926374h.
URL https://pubs.rsc.org/en/content/articlehtml/2010/jm/b926374hhttps://pubs.rsc.org/en/content/articlelanding/2010/jm/b926374h

[31] M. Nakata, G. Zanchetta, B. D. Chapman, C. D. Jones, J. O. Cross, R. Pindak, T. Bellini, N. A. Clark, End-to-end stacking and liquid crystal condensation of 6-to 20-base pair DNA duplexes, Science 318 (5854) (2007) 1276–1279. doi:10.1126/science.1143826.
URL https://pubmed.ncbi.nlm.nih.gov/18033877/

[32] T. P. Fraccia, G. P. Smith, L. Bethge, G. Zanchetta, G. Nava, S. Klussmann, N. A. Clark, T. Bellini, Liquid Crystal Ordering and Isotropic Gelation in Solutions of Four-Base-Long DNA Oligomers, ACS Nano 10 (9) (2016) 8508–8516. doi:10.1021/acsnano.6b03622.
URL www.acsnano.org

[33] G. P. Smith, T. P. Fraccia, M. Todisco, G. Zanchetta, C. Zhu, E. Hayden, T. Bellini, N. A. Clark, Backbone-free duplex-stacked monomer nucleic acids exhibiting Watson–Crick selectivity, Proceedings of the National Academy of Sciences of the United States of America 115 (33) (2018) E7658–E7664. doi:10.1073/pnas.1721369115.
URL https://www.pnas.org/content/115/33/E7658https://www.pnas.org/content/115/33/E7658.abstract

[34] V. Jamali, N. Behabtu, B. Senyuk, J. A. Lee, I. I. Smalyukh, P. Van Der Schoot, M. Pasquali, Experimental realization of crossover in shape and director field of nematic tactoids, Physical Review E - Statistical, Nonlinear, and Soft Matter Physics 91 (4) (4 2015). doi:10.1103/PhysRevE.91.042507.

[35] J. Viamontes, P. W. Oakes, J. X. Tang, Isotropic to nematic liquid crystalline phase transition of F-actin varies from continuous to first oder, Physical Review Letters 97 (11) (2006). doi:10.1103/PhysRevLett.97.118103.

[36] P. X. Wang, M. J. MacLachlan, Liquid crystalline tactoids: Ordered structure, defective coalescence and evolution in confined geometries (2 2018). doi:10.1098/rsta.2017.0042.

[37] M. P. Taylor, J. Herzfeld, A Model for Nematic and Columnar Ordering in a Self-Assembling System*, Tech. rep. (1990).
URL https://pubs.acs.org/sharingguidelines

[38] A. Speranza, P. Sollich, Simplified Onsager theory for isotropic-nematic phase equilibria of length polydisperse hard rods, Journal of Chemical Physics 117 (11) (2002) 5421–5436. doi:10.1063/1.1499718.
URL http://scitation.aip.org/content/aip/journal/jcp/117/11/10.1063/1.1499718

[39] P. J. Flory, Themodynamics of high polymer solutions, The Journal of Chemical Physics 10 (1) (1942) 51–61. doi:10.1063/1.1723621.

[40] M. L. Huggins, Some Properties of Solutions of Long-chain Compounds., The Journal of Physical Chemistry 46 (1) (1942) 151–158. doi:10.1021/j150415a018.
URL https://doi.org/10.1021/j150415a018

[41] C. E. Sing, S. L. Perry, Recent progress in the science of complex coacervation, Soft Matter 16 (12) (2020) 2885–2914. doi:10.1039/d0sm00001a.

[42] J. R. Vieregg, M. Lueckheide, A. B. Marciel, L. Leon, A. J. Bologna, J. R. Rivera, M. V. Tirrell, Oligonucleotide-peptide complexes: Phase control by hybridization, Journal of the American Chemical Society 140 (5) (2018) 1632–1638. doi:10.1021/jacs.7b03567.

[43] A. M. Rumyantsev, E. B. Zhulina, O. V. Borisov, Complex Coacervate of Weakly Charged Polyelectrolytes: Diagram of States, Macromolecules 51 (10) (2018) 3788–3801. doi:10.1021/acs.macromol.8b00342.

[44] A. M. Rumyantsev, J. J. De Pablo, Liquid Crystalline and Isotropic

Coacervates of Semiflexible Polyanions and Flexible Polycations, Macromolecules 52 (14) (2019) 5140–5156. doi:10.1021/acs.macromol.9b00797.

[45] S. Di Leo, M. Todisco, T. Bellini, T. P. Fraccia, Phase separations, liquid crystal ordering and molecular partitioning in mixtures of PEG and DNA oligomers, Liquid Crystals 45 (13-15) (2018) 2306–2318. doi:10.1080/02678292.2018.1519123.

[46] T. P. Fraccia, G. P. Smith, G. Zanchetta, E. Paraboschi, Y. Yi, D. M. Walba, G. Dieci, N. A. Clark, T. Bellini, Abiotic ligation of DNA oligomers templated by their liquid crystal ordering, Nature Communications 6 (3 2015). doi:10.1038/ncomms7424.

[47] L. S. Lerman, A transition to a compact form of DNA in polymer solutions., Proceedings of the National Academy of Sciences of the United States of America 68 (8) (1971) 1886–1890. doi:10.1073/pnas.68.8.1886.
URL https://www.pnas.org/content/68/8/1886https://www.pnas.org/content/68/8/1886.abstract

[48] V. A. Bloomfield, DNA condensation, Current Opinion in Structural Biology 6 (3) (1996) 334–341.

[49] H. H. Strey, V. A. Parsegian, R. Podgornik, Equation of state for dna liquid crystals: Fluctuation enhanced electrostatic double layer repulsion, Physical Review Letters 78 (5) (1997) 895–898. doi:10.1103/PhysRevLett.78.895.
URL https://journals.aps.org/prl/abstract/10.1103/PhysRevLett.78.895

[50] S. Yasar, R. Podgornik, J. Valle-Orero, M. R. Johnson, V. A. Parsegian, Continuity of states between the cholesteric → line hexatic transition and the condensation transition in DNA solutions, Scientific Reports 4 (11 2014). doi:10.1038/srep06877.

[51] G. Zanchetta, M. Nakata, M. Buscaglia, T. Bellini, N. A. Clark, Phase separation and liquid crystallization of complementary sequences in mixtures of nanoDNA oligomers, Proceedings of the National Academy of Sciences of the United States of America 105 (4) (2008) 1111–1117. doi:10.1073/pnas.0711319105.
URL https://www.pnas.org/content/105/4/1111https://www.pnas.org/content/105/4/1111.abstract

[52] G. Zanchetta, M. Nakata, M. Buscaglia, N. A. Clark, T. Bellini, Liquid crystal ordering of DNA and RNA oligomers with partially overlapping sequences, Journal of Physics Condensed Matter 20 (49) (2008) 494214. doi:10.1088/0953-8984/20/49/494214.
URL https://iopscience.iop.org/article/10.1088/0953-8984/20/49/494214https://iopscience.iop.org/article/10.1088/0953-8984/20/49/494214/meta

[53] T. Kuriabova, M. D. Betterton, M. A. Glaser, Linear aggregation and liquid-crystalline order: Comparison of Monte Carlo simulation and analytic theory, Journal of Materials Chemistry 20 (46) (2010) 10366–10383. doi:10.1039/c0jm02355h.
URL https://pubs.rsc.org/en/content/articlehtml/2010/jm/c0jm02355hhttps://pubs.rsc.org/en/content/articlelanding/2010/jm/c0jm02355h

[54] T. Bellini, G. Zanchetta, T. P. Fraccia, R. Cerbino, E. Tsai, G. P. Smith, M. J. Moran, D. M. Walba, N. A. Clark, Liquid crystal self-assembly of random-sequence DNA oligomers, Proceedings of the National Academy of Sciences of the United States of America 109 (4) (2012) 1110–1115. doi:10.1073/pnas.1117463109.
URL www.pnas.org/cgi/doi/10.1073/pnas.1117463109

[55] W. Guo, A. B. Kinghorn, Y. Zhang, Q. Li, A. D. Poonam, J. A. Tanner, H. C. Shum, Non-associative phase separation in an evaporating droplet as a model for prebiotic compartmentalization, Nature Communications 12 (1) (2021) 3194. doi:10.1038/s41467-021-23410-7.
URL http://www.nature.com/articles/s41467-021-23410-7

[56] M. Todisco, T. P. Fraccia, G. P. Smith, A. Corno, L. Bethge, S. Klussmann, E. M. Paraboschi, R. Asselta, D. Colombo, G. Zanchetta, N. A. Clark, T. Bellini, Nonenzymatic Polymerization into Long Linear RNA Templated by Liquid Crystal Self-Assembly, ACS Nano (2018). doi:10.1021/acsnano.8b05821.

[57] T. Z. Jia, T. P. Fraccia, Liquid crystal peptide/DNA coacervates in the context of prebiotic molecular evolution, Crystals 10 (11) (2020) 1–21. doi:10.3390/cryst10110964.

[58] T. P. Fraccia, T. Z. Jia, Liquid crystal coacervates composed of short double-stranded DNA and cationic peptides, ACS Nano 14 (11) (2020) 15071–15082. doi:10.1021/acsnano.0c05083.

[59] X. Liu, M. Haddou, I. Grillo, Z. Mana, J. P. Chapel, C. Schatz, Early stage kinetics of polyelectrolyte complex coacervation monitored through stopped-flow light scattering, Soft Matter 12 (44) (2016) 9030–9038. doi:10.1039/c6sm01979j.

[60] O. Lambert, L. Letellier, W. M. Gelbart, J.-L. Rigaud, M. F. Hawthorne, DNA delivery by phage as a strategy for encapsulating toroidal condensates of arbitrary size into liposomes, Tech. rep.
URL www.pnas.org

[61] J.-L. Sikorav, J. Pelta, F. Livolant, A Liquid Crystalline Phase in Spermidine-Condensed DNA, Tech. rep. (1994).

[62] J. Pelta, F. Oise Livolant, J.-L. Sikorav, DNA Aggregation Induced by Polyamines and Cobalthexamine*, Tech. rep. (1996).

[63] E. Raspaud, D. Durand, F. Livolant, Interhelical spacing in liquid crystalline spermine and spermidine-DNA precipitates, Biophysical Journal 88 (1) (2005) 392–403. doi:10.1529/biophysj.104.040113.

[64] X. Qiu, K. Andresen, J. S. Lamb, L. W. Kwok, L. Pollack, Abrupt transition from a free, repulsive to a condensed, attractive DNA phase, induced by multivalent polyamine cations, Physical Review Letters 101 (22) (11 2008). doi:10.1103/PhysRevLett.101.228101.

[65] S. Alberti, A. Gladfelter, T. Mittag, Considerations and Challenges in Studying Liquid-Liquid Phase Separation and Biomolecular Condensates, Cell 176 (3) (2019) 419–434. doi:10.1016/j.cell.2018.12.035.
URL https://doi.org/10.1016/j.cell.2018.12.035

[66] A. Shakya, J. T. King, DNA Local-Flexibility-Dependent Assembly of Phase-Separated Liquid Droplets, Biophysical Journal 115 (10) (2018) 1840–1847. doi:10.1016/j.bpj.2018.09.022.

[67] X. Liu, J. P. Chapel, C. Schatz, Structure, thermodynamic and kinetic signatures of a synthetic polyelectrolyte coacervating system (1 2017). doi:10.1016/j.cis.2016.10.004.

[68] W. C. Blocher McTigue, E. Voke, L. W. Chang, S. L. Perry, The benefit of poor mixing: Kinetics of coacervation, Physical Chemistry Chemical Physics 22 (36) (2020) 20643–20657. doi:10.1039/d0cp03224g.

[69] F. Muzzopappa, M. Hertzog, F. Erdel, DNA length tunes the fluidity of DNA-based condensates, Biophysical Journal 120 (7) (2021) 1288–1300. doi:10.1016/j.bpj.2021.02.027.

[70] H. S. Park, S. W. Kang, L. Tortora, S. Kumar, O. D. Lavrentovich, Condensation of self-assembled lyotropic chromonic liquid crystal sunset yellow in aqueous solutions crowded with polyethylene glycol and doped with salt, Langmuir 27 (7) (2011) 4164–4175. doi:10.1021/la200505y.

[71] H. Lee, V. Sunkara, Y. K. Cho, J. Jeong, Effects of poly(ethylene glycol) on the wetting behavior and director configuration of lyotropic chromonic liquid crystals confined in cylinders, Soft Matter 15 (30) (2019) 6127–6133. doi:10.1039/c9sm00927b.

[72] K. A. Simon, P. Sejwal, R. B. Gerecht, Y. Y. Luk, Water-in-water emulsions stabilized by non-amphiphilic interactions: Polymer-dispersed lyotropic liquid crystals, Langmuir 23 (3) (2007) 1453–1458. doi:10.1021/la062203s.
URL https://pubs.acs.org/sharingguidelines

[73] L. Tortora, H. S. Park, S. W. Kang, V. Savaryn, S. H. Hong, K. Kaznatcheev, D. Finotello, S. Sprunt, S. Kumar, O. D. Lavrentovich, Self-assembly, condensation, and order in aqueous lyotropic chromonic liquid crystals crowded with additives, Soft Matter 6 (17) (2010) 4157–4167. doi:10.1039/c0sm00065e.

[74] R. Koizumi, B. X. Li, O. D. Lavrentovich, Effect of crowding agent polyethylene glycol on lyotropic chromonic liquid crystal phases of disodium cromoglycate, Crystals 9 (3) (3 2019). doi:10.3390/cryst9030160.

[75] A. Yamaguchi, G. P. Smith, Y. Yi, C. Xu, S. Biffi, F. Serra, T. Bellini, C. Zhu, N. A. Clark, Phases and structures of sunset yellow and disodium cromoglycate mixtures in water, Physical Review E 93 (1) (1 2016). doi:10.1103/PhysRevE.93.012704.

[76] H. S. Park, S. W. Kang, L. Tortora, Y. Nastishin, D. Finotello, S. Kumar, O. D. Lavrentovieh, Self-assembly of Lyotropic chromonic liquid crystal sunset yellow and effects of ionic additives, Journal of Physical Chemistry B 112 (51) (2008) 16307–16319. doi:10.1021/jp804767z.

[77] A. P. Ormerod, J. W. Jones, H. Wheatcroft, A. Alfutimie, G. J. Tiddy, The influence of polar additives on chromonic mesophase formation of Edicol Sunset Yellow, Liquid Crystals 42 (5-6) (2015) 772–782. doi:

10.1080/02678292.2014.992377.

[78] D. Miyoshi, A. Nakao, N. Sugimoto, Molecular crowding regulates the structural switch of the DNA G-quadruplex, Biochemistry 41 (50) (2002) 15017–15024. doi:10.1021/bi020412f.

[79] M. Trajkovski, T. Endoh, H. Tateishi-Karimata, T. Ohyama, S. Tanaka, J. Plavec, N. Sugimoto, Pursuing origins of (poly)ethylene glycol-induced G-quadruplex structural modulations, Nucleic Acids Research 46 (8) (2018) 4301–4315. doi:10.1093/nar/gky250.

[80] M. Mimura, S. Tomita, Y. Shinkai, T. Hosokai, H. Kumeta, T. Saio, K. Shiraki, R. Kurita, Quadruplex Folding Promotes the Condensation of Linker Histones and DNAs via Liquid–Liquid Phase Separation, Journal of the American Chemical Society (2021) jacs.1c03447doi:10.1021/jacs.1c03447.
URL https://pubs.acs.org/doi/10.1021/jacs.1c03447

[81] P. Mariani, L. Saturni, Measurement of intercolumnar forces between parallel guanosine four-stranded helices, Biophysical Journal 70 (6) (1996) 2867–2874. doi:10.1016/S0006-3495(96)79856-9.

[82] T. Lu, K. K. Nakashima, E. Spruijt, Temperature-Responsive Peptide-Nucleotide Coacervates, Journal of Physical Chemistry B 125 (12) (2021) 3080–3091. doi:10.1021/acs.jpcb.0c10839.

[83] Y. Xu, A. D. Atrens, J. R. Stokes, Liquid crystal hydroglass formed via phase separation of nanocellulose colloidal rods, Soft Matter 15 (8) (2019) 1716–1720. doi:10.1039/C8SM02288G.

[84] H. Oguzlu, I. Dobyrden, X. Liu, S. Bhaduri, P. M. Claesson, Y. Boluk, Polymer Induced Gelation of Aqueous Suspensions of Cellulose Nanocrystals, Langmuir 37 (10) (2021) 3015–3024. doi:10.1021/acs.langmuir.0c02336.

[85] R. M. Parker, B. Frka-Petesic, G. Guidetti, G. Kamita, G. Consani, C. Abell, S. Vignolini, Hierarchical Self-Assembly of Cellulose Nanocrystals in a Confined Geometry, ACS Nano 10 (9) (2016) 8443–8449. doi:10.1021/acsnano.6b03355.

[86] J. P. Lagerwall, C. Schütz, M. Salajkova, J. Noh, J. H. Park, G. Scalia, L. Bergström, Cellulose nanocrystal-based materials: From liquid crystal self-assembly and glass formation to multifunctional thin films (1 2014). doi:10.1038/am.2013.69.
URL www.nature.com/am

[87] P. Bertsch, S. Isabettini, P. Fischer, Ion-Induced Hydrogel Formation and Nematic Ordering of Nanocrystalline Cellulose Suspensions, Biomacromolecules 18 (12) (2017) 4060–4066. doi:10.1021/acs.biomac.7b01119.

[88] C. Honorato-Rios, C. Lehr, C. Schütz, R. Sanctuary, M. A. Osipov, J. Baller, J. P. Lagerwall, Fractionation of cellulose nanocrystals: enhancing liquid crystal ordering without promoting gelation, NPG Asia Materials 10 (5) (2018) 455–465. doi:10.1038/s41427-018-0046-1.

[89] J. R. Bruckner, A. Kuhnhold, C. Honorato-Rios, T. Schilling, J. P. Lagerwall, Enhancing self-assembly in cellulose nanocrystal suspensions using high-permittivity solvents, Langmuir 32 (38) (2016) 9854–9862. doi:10.1021/acs.langmuir.6b02647.

[90] G. Chu, G. Vasilyev, D. Qu, S. Deng, L. Bai, O. J. Rojas, E. Zussman, Structural Arrest and Phase Transition in Glassy Nanocellulose Colloids, Langmuir 36 (4) (2020) 979–985. doi:10.1021/acs.langmuir.9b03570.

[91] C. D. Edgar, D. G. Gray, Influence of dextran on the phase behavior of suspensions of cellulose nanocrystals, Macromolecules 35 (19) (2002) 7400–7406. doi:10.1021/ma0204195.

[92] H. Oguzlu, Y. Boluk, Interactions between cellulose nanocrystals and anionic and neutral polymers in aqueous solutions, Cellulose 24 (1) (2017) 131–146. doi:10.1007/s10570-016-1096-6.

[93] B. Peng, J. Tang, P. Wang, J. Luo, P. Xiao, Y. Lin, K. C. Tam, Rheological properties of cellulose nanocrystal-polymeric systems, Cellulose 25 (6) (2018) 3229–3240. doi:10.1007/s10570-018-1775-6.

[94] J. Jeong, Z. S. Davidson, P. J. Collings, T. C. Lubensky, A. G. Yodh, Chiral symmetry breaking and surface faceting in chromonic liquid crystal droplets with giant elastic anisotropy, Proceedings of the National Academy of Sciences of the United States of America 111 (5) (2014) 1742–1747. doi:10.1073/pnas.1315121111.

[95] K. L. Weirich, S. Banerjee, K. Dasbiswas, T. A. Witten, S. Vaikuntanathan, M. L. Gardel, Liquid behavior of cross-linked actin bundles, Proceedings of the National Academy of Sciences of the United States of America 114 (9) (2017) 2131–2136. doi:10.1073/pnas.1616133114.

[96] D. R. Scheff, D. R. Scheff, K. L. Weirich, K. L. Weirich, K. L. Weirich, K. Dasbiswas, A. Patel, A. Patel, S. Vaikuntanathan, S. Vaikuntanathan, M. L. Gardel, M. L. Gardel, M. L. Gardel, M. L. Gardel, Tuning shape and internal structure of protein droplets: Via biopolymer filaments, Soft Matter 16 (24) (2020) 5659–5668. doi:10.1039/c9sm02462j.

[97] A. Modlinska, A. M. Alsayed, T. Gibaud, Condensation and dissolution of nematic droplets in dispersions of colloidal rods with thermo-sensitive depletants, Scientific Reports 5 (12 2015). doi:10.1038/srep18432.

[98] J. Alvarado, B. M. Mulder, G. H. Koenderink, Alignment of nematic and bundled semiflexible polymers in cell-sized confinement, Soft Matter 10 (14) (2014) 2354–2364. doi:10.1039/c3sm52421c.
URL www.softmatter.org

[99] Y. Mulla, F. C. Mackintosh, G. H. Koenderink, Origin of Slow Stress Relaxation in the Cytoskeleton, Physical Review Letters 122 (21) (2019) 218102. doi:10.1103/PhysRevLett.122.218102.
URL https://journals.aps.org/prl/abstract/10.1103/PhysRevLett.122.218102

[100] M. Siavashpouri, C. H. Wachauf, M. J. Zakhary, F. Praetorius, H. Dietz, Z. Dogic, Molecular engineering of chiral colloidal liquid crystals using DNA origami (2017) 22doi:10.1038/NMAT4909.
URL www.nature.com/naturematerials

[101] Z. Dogic, K. R. Purdy, E. Grelet, M. Adams, S. Fraden, Isotropic-nematic phase transition in suspensions of filamentous virus and the neutral polymer Dextran, Physical Review E - Statistical Physics, Plasmas, Fluids, and Related Interdisciplinary Topics 69 (5) (2004) 9. doi:10.1103/PhysRevE.69.051702.
URL https://journals.aps.org/pre/abstract/10.1103/PhysRevE.69.051702

[102] T. Gibaud, E. Barry, M. J. Zakhary, M. Henglin, A. Ward, Y. Yang, C. Berciu, R. Oldenbourg, M. F. Hagan, D. Nicastro, R. B. Meyer, Z. Dogic, Reconfigurable self-assembly through chiral control of interfacial tension (2012). doi:10.1038/nature10769.

[103] C. R. Bridges, M. J. Ford, B. C. Popere, G. C. Bazan, R. A. Segalman, Formation and Structure of Lyotropic Liquid Crystalline Mesophases in Donor-Acceptor Semiconducting Polymers, Macromolecules 49 (19) (2016) 7220–7229. doi:10.1021/acs.macromol.6b01650.

[104] W. J. Yoon, Y. J. Choi, D. G. Kang, D. Y. Kim, M. Park, J. H. Lee, S. W. Kang, S. H. Lee, K. U. Jeong, Construction of Polymer-Stabilized Automatic MultiDomain Vertical Molecular Alignment Layers with Pretilt Angles by Photopolymerizing Dendritic Monomers under Electric Fields, ACS Omega 2 (9) (2017) 5942–5948. doi:10.1021/acsomega.7b01015.

[105] D. Y. Kim, S. I. Lim, D. Jung, J. K. Hwang, N. Kim, K. U. Jeong, Self-assembly and polymer-stabilization of lyotropic liquid crystals in aqueous and non-aqueous solutions (1 2017). doi:10.1080/21680396.2017.1327827.

[106] L. Lucchetti, T. Fraccia, F. Ciciulla, F. Simoni, T. Bellini, Giant optical nonlinearity in DNA lyotropic liquid crystals, Optics Express 25 (21) (2017). doi:10.1364/OE.25.025951.

[107] L. Lucchetti, T. P. Fraccia, G. Nava, T. Turiv, F. Ciciulla, L. Bethge, S. Klussmann, O. D. Lavrentovich, T. Bellini, Elasticity and Viscosity of DNA Liquid Crystals, ACS Macro Letters 9 (7) (2020) 1034–1039. doi:10.1021/acsmacrolett.0c00394.

[108] T. Lu, E. Spruijt, Multiphase Complex Coacervate Droplets, Journal of the American Chemical Society 142 (6) (2020) 2905–2914. doi:10.1021/jacs.9b11468.

[109] J. Deng, A. Walther, Programmable ATP-Fueled DNA Coacervates by Transient Liquid-Liquid Phase Separation, Chem 6 (12) (2020) 3329–3343. doi:10.1016/j.chempr.2020.09.022.

[110] Z. Reich, E. Wachtel, A. Minsky, Liquid-crystalline mesophases of plasmid DNA in bacteria, Science 264 (5164) (1994) 1460–1463. doi:10.1126/science.8197460.

[111] H. Almohammadi, M. Bagnani, R. Mezzenga, Flow-induced order–order transitions in amyloid fibril liquid crystalline tactoids, Nature Communications 11 (1) (12 2020). doi:10.1038/s41467-020-19213-x.

[112] G. Nyström, M. Arcari, R. Mezzenga, Confinement-induced liquid crystalline transitions in amyloid fibril cholesteric tactoids, Nature Nanotechnology 13 (4) (2018) 330–336. doi:10.1038/s41565-018-0071-9.

[113] R. F. Berkeley, M. Kashefi, G. T. Debelouchina, Real-time observation of structure and dynamics during the liquid-to-solid transition of FUS LC, Biophysical Journal 120 (7) (2021) 1276–1287. doi:10.1016/j.bpj.2021.02.008.

[114] E. Chuang, A. M. Hori, C. D. Hesketh, J. Shorter, Amyloid assembly and disassembly (4 2018). doi:10.1242/jcs.189928.

[115] J. W. Smith, X. Jiang, H. An, A. M. Barclay, G. Licari, E. Tajkhorshid, E. G. Moore, C. M. Rienstra, J. S. Moore, Q. Chen, Polymer-Peptide Conjugates Convert Amyloid into Protein Nanobundles through Fragmentation and Lateral Association, ACS Applied Nano Materials 3 (2) (2020) 937–945. doi:10.1021/acsanm.9b01331.